

# $B$ -to-Glueball form factor and Glueball production in $B$ decays

Wei Wang<sup>a</sup>, Yue-Long Shen<sup>b,c</sup> and Cai-Dian Lü<sup>a</sup>

<sup>a</sup> *Institute of High Energy Physics and Theoretical Physics Center for Science Facilities,  
Chinese Academy of Sciences, Beijing 100049, People's Republic of China*

<sup>b</sup> *Institute of Physics, Academia Sinica, Taipei, Taiwan 115, Republic of China*

<sup>c</sup> *College of Information Science and Engineering, Ocean University of China,  
Qingdao, Shandong 266100, People's Republic of China*

We investigate transition form factors of  $B$  meson decays into a scalar glueball in the light-cone formalism. Compared with form factors of  $B$  to ordinary scalar mesons, the  $B$ -to-glueball form factors have the same power in the expansion of  $1/m_B$ . Taking into account the leading twist light-cone distribution amplitude, we find that they are numerically smaller than those form factors of  $B$  to ordinary scalar mesons. Semileptonic  $B \rightarrow Gl\bar{\nu}$ ,  $B \rightarrow Gl^+l^-$  and  $B_s \rightarrow Gl^+l^-$  decays are subsequently investigated. We also analyze the production rates of scalar mesons in semileptonic  $B$  decays in the presence of mixing between scalar  $\bar{q}q$  and glueball states. The glueball production in  $B_c$  meson decays is also investigated and the LHCb experiment may discover this channel. The sizable branching fraction in  $B_c \rightarrow (\pi^+\pi^-)l^-\bar{\nu}$ ,  $B_c \rightarrow (K^+K^-)l^-\bar{\nu}$  or  $B_c \rightarrow (\pi^+\pi^-\pi^+\pi^-)l^-\bar{\nu}$  could be a clear signal for a scalar glueball state.

PACS numbers: 13.25.Hw, 12.39.Ki

## I. INTRODUCTION

The existence of the glueball state is permitted by the QCD. Based on the valence approximation, Lattice QCD calculations have predicted that the mass of the lowest-lying scalar glueball is around 1.5-1.8 GeV [1, 2]. Many different candidates have been observed in this mass region, but there is not any solid evidence on the existence of a pure glueball. It is very likely that the glueball mixes with the quark-antiquark state and they together form several physical mesons. On the theoretical side, there are large ambiguities on the mixing mechanism, please see Ref. [3] for a review on the status.

Most studies focus on the decay property of the glueball. In fact, the production property of the glueball is an alternative way to uncover the mysterious structure of scalar mesons and figure out the gluon component inside. In  $B$  meson decays, the color magnetic operator  $O_{8g}$  has a large Wilson coefficient that could produce a number of gluons easily. These gluons in the final state may have the tendency to form a glue state, thus the glueball production in inclusive  $B$  decays has attracted some theoretical interests [4, 5]. The authors in Ref. [6] have also studied the exclusive  $B \rightarrow KG$  and  $B \rightarrow K^*G$  decays, where  $G$  is a scalar glueball. Based on the results in Ref. [7], they have neglected gluon recoiled Feynman diagrams and studied the contributions, in which a scalar glueball state is emitted and a  $K$  or  $K^*$  meson is recoiled.

In the present paper, we study the transition form factors of  $B$  decays into a scalar glueball and point out another interesting mechanism to detect a glueball via the exclusive  $B$  decays. These form factors are relevant for productions of scalar glueballs in semileptonic  $B$  decays. Up to the leading Fock state and leading order in  $\alpha_s$ , there are three different Feynman diagrams shown in Fig. 1. Since the two gluons bounded in a glueball state are already symmetrized in the glueball wave function, it is not necessary to consider the crossed diagram. The first diagram is similar with the one studied in Ref. [7]. Through the power counting rule, we will show that the first two diagrams have the same power with the  $B$ -to-light meson form factors. That will affect numerical results of the transition form factors and production rates in semileptonic  $B$  decays.

The ordinary light neutral scalar meson is isospin singlet and/or flavor SU(3) singlet, while the glueball is flavor

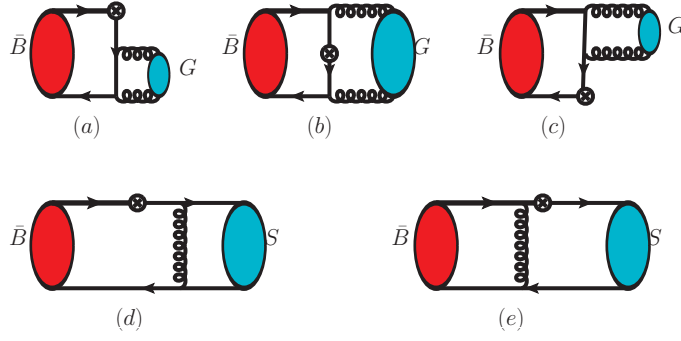


FIG. 1: Feynman diagrams of  $\bar{B}$  decays into a scalar glueball  $G$  (first row) and an ordinary scalar meson (second row). The  $\otimes$  denotes the possible Lorentz structure arising from the electroweak interactions.

SU(6) singlet. Therefore it is difficult to distinguish them by the light  $u$ ,  $d$  and  $s$  quark coupling. However, the light ordinary scalar meson has negligible  $c\bar{c}$  component, while the glueball have the same coupling to  $c\bar{c}$  as that to the  $u\bar{u}$ ,  $d\bar{d}$  or  $s\bar{s}$ . A clean way to identify a glueball is then through the  $c\bar{c}$  coupling to the glueball. We briefly analyze the production in  $B_c$  meson decays.

The paper is organized as follows. In section II, we give the analysis of the power counting of the  $B \rightarrow G$  transition form factors. In the perturbative QCD (PQCD) approach [8, 9], the form factors are calculated in the section III. Numerical results and detailed discussions will be presented in the subsequent section. We also briefly analyze the discussion in  $B_c$  meson decays. We conclude in the last section. Functions used in the PQCD approach are collected in the appendix.

## II. POWER COUNTING OF TRANSITION FORM FACTORS

Transition form factors of  $B$  decays into scalar mesons are defined by

$$\begin{aligned}
 \langle S(P_S) | \bar{q} \gamma_\mu \gamma_5 b | \bar{B}(P_B) \rangle &= -i \left\{ \left[ (P_B + P_S)_\mu - \frac{m_B^2 - m_S^2}{q^2} q_\mu \right] F_1(q^2) + \frac{m_B^2 - m_S^2}{q^2} q_\mu F_0(q^2) \right\}, \\
 \langle S(P_S) | \bar{q} \sigma_{\mu\nu} b | \bar{B}(P_B) \rangle &= i \epsilon_{\mu\nu\alpha\beta} P_S^\alpha q^\beta \frac{2F_T(q^2)}{m_B + m_S}, \\
 \langle S(P_S) | \bar{q} \sigma_{\mu\nu} \gamma_5 b | \bar{B}(P_B) \rangle &= -\frac{F_T(q^2)}{m_B + m_S} [(P_B + P_S)_\mu q_\nu - q_\mu (P_B + P_S)_\nu],
 \end{aligned} \tag{1}$$

where  $S$  denotes an ordinary scalar meson or a scalar glueball.  $q = P_B - P_S$  and  $m_B(m_S)$  is the mass of the  $B$  (scalar) meson.

In the following, we will work in the rest frame of the  $B$  meson and use light-cone coordinates. In the heavy quark limit, the mass difference between  $b$  quark ( $m_b$ ) and  $B$  meson ( $m_B$ ) is negligible. The mass of a light glueball is small compared with the  $b$  quark mass, thus in the transition amplitudes we keep them up to the leading order. Since the scalar glueball in the final state moves very fast in the large-recoil region, we choose its momentum mainly on the plus direction in the light-cone coordinates. The momentum of  $B$  meson and the light scalar meson can be denoted as

$$P_B = \frac{m_B}{\sqrt{2}}(1, 1, 0_\perp), \quad P_2 = \frac{m_B}{\sqrt{2}}(\rho, 0, 0_\perp). \tag{2}$$

The momentum transfer is  $q = P_B - P_2$ , and there exists the relation  $\rho \approx 1 - q^2/m_B^2$ .

In the expansion on  $\alpha_s$ , the lowest order Feynman diagrams for form factors of  $B$  decays into a scalar glueball are depicted in Fig. 1. Up to the leading Fock state, two gluons should be generated to form a glueball. In exclusive  $B$  decays, these two gluons can be emitted from either the heavy  $b$  quark or the light quark. The  $\otimes$  in Fig. 1 denotes the weak vertices. Momentum fractions of the light antiquark in  $B$  meson and the upper (lower) gluon depicted in Fig 1 are denoted as  $x_1$  and  $x_2$  ( $\bar{x}_2 = 1 - x_2$ ), respectively.

In the first diagram of Fig. 1, each of the two internal quark propagators is the sum of a collinear momentum (gluon) and a soft momentum (light quark). The virtualities of them are of order  $\Lambda_{\text{QCD}}m_b$ , where  $\Lambda_{\text{QCD}}$  is the hadronic scale. In the second and the third diagram, one or two light propagators become heavy  $b$  quark propagators, whose virtualities become  $m_b^2$  instead of  $\Lambda_{\text{QCD}}m_b$ . Superficially, one may conclude that the power counting for the three diagrams obey the relation:  $F(a) > F(b) > F(c)$ . But in fact, this relation is not exactly correct. As we will show in the following, the leading twist light-cone distribution amplitude is constructed in the case that the two gluons are transversely polarized. So the structures of the vertices attaching to these two gluons in the first diagram have the form:  $\gamma_{\perp}^{\mu}$ . Apparently, the numerator of the propagators commutes with the transverse Dirac matrix. So, the amplitude is proportional to  $(\bar{x}_2 \not{P}_2 - x_1 \not{P}_B)(\not{P}_2 - x_1 \not{P}_B) \approx -x_1 \not{P}_B \not{P}_2 - x_1 \bar{x}_2 \not{P}_2 \not{P}_B$ . We can see that neglecting the glueball's mass square, there is a small momentum fraction  $x_1$  in the numerator, which will cancel one of the momentum fraction of the denominator. The effective power for one light propagator in the first diagram becomes  $m_b^2$ , which is the same as a heavy propagator in the second diagram. It implies:  $F(a) \sim F(b) > F(c)$ . Adopting the power counting rule for the  $B$  meson wave function and the scaling behaviors for the distribution amplitudes of collinear meson, given in Ref. [10], we directly obtain

$$F^{B \rightarrow G} \sim \alpha_s (\sqrt{m_b \Lambda_{\text{QCD}}}) \left( \frac{\Lambda_{\text{QCD}}}{m_b} \right)^{3/2}, \quad (3)$$

where the form factor is dominated by the first two diagrams. The  $B \rightarrow G$  form factors have the same scaling rule with the  $B$ -to-light transition form factor. And we can expect that the gluonic  $B \rightarrow \eta$  form factors also obey this rule. While the light-cone distribution amplitude of a gluonic pseudo-scalar meson is normalized to zero, only the higher Gegenbauer moments contribute. The first effective Gegenbauer moment of  $\eta$  and  $\eta'$  is very small, so the gluonic contribution to  $B \rightarrow \eta$  form factors is found to be numerically small [7].

Since these diagrams are free of the endpoint singularity, both collinear factorization and  $k_T$  factorization are applicable. In the following, we will use the perturbative QCD approach to investigate the transition form factors, where the inclusion of the transverse momentum only improves the theoretical precision.

### III. TRANSITION FORM FACTORS IN THE PERTURBATIVE QCD APPROACH

$B$  meson is a heavy-light system, whose light-cone matrix element can be decomposed as [11, 12]

$$\int_0^1 \frac{d^4 z}{(2\pi)^4} e^{ik_1 \cdot z} \langle 0 | b_{\beta}(0) \bar{q}_{\alpha}(z) | \bar{B}(P_B) \rangle = \frac{i}{\sqrt{2N_c}} \left\{ (P_B + m_B) \gamma_5 \left[ \phi_B(k_1) + \frac{\not{v}}{\sqrt{2}} \bar{\phi}_B(k_1) \right] \right\}_{\beta\alpha}, \quad (4)$$

where  $n = (1, 0, \mathbf{0}_T)$  and  $v = (0, 1, \mathbf{0}_T)$  are light-like unit vectors. There are two Lorentz structures in  $B$  meson light-cone distribution amplitudes, and they obey the normalization conditions:

$$\int \frac{d^4 k_1}{(2\pi)^4} \phi_B(k_1) = \frac{f_B}{2\sqrt{2N_c}}, \quad \int \frac{d^4 k_1}{(2\pi)^4} \bar{\phi}_B(k_1) = 0, \quad (5)$$

with  $f_B$  as the decay constant of  $B$  meson.

In principle, both the  $\phi_B(k_1)$  and  $\bar{\phi}_B(k_1)$  contribute in  $B$  meson decays. For  $B$ -to-glueball transition, the  $\bar{\phi}_B(k_1)$  can be neglected in the second diagram. The amplitude for the form factors is obtained by evaluating the trace of

the wave functions and the scattering kernels. As we will show in the following, the gluon in a glueball is transversely polarized at the leading power. So the Lorentz structure  $\not{n}$  for the wave function  $\bar{\phi}_B(k_1)$  commutes with the gluon vertex and encounters the propagator  $(\bar{x}_2 \not{P}_2 - x_1 \not{P}_B)$ . The momentum of the glueball is parallel with this direction  $n$ , thus the nonzero term contains a factor  $x_1$  and is naturally power suppressed. For the other diagrams, we do not find any analytical reason to neglect the distribution amplitude  $\bar{\phi}_B(k_1)$ . The computation depends on the shape of this distribution amplitude but it is not well constrained in the PQCD approach at present. In fact, including the  $\bar{\phi}_B(k_1)$  term will not improve the quality of the calculation significantly, but introduce one more free parameter. Nevertheless in  $B$  decays into ordinary  $\bar{q}q$  mesons the contribution of  $\bar{\phi}_B(k_1)$  is usually neglected, because its contribution is numerically small in the PQCD approach [13, 14]. We will keep the term with  $\phi_B(k_1)$  in equation (4) in this work and leave the term with  $\bar{\phi}_B(k_1)$  in a future study. In the momentum space the light cone matrix of  $B$  meson can be expressed as:

$$\Phi_B = \frac{i}{\sqrt{6}}(\not{P}_B + m_B)\gamma_5\phi_B(k_1). \quad (6)$$

Usually the hard part is independent of  $k^+$  or/and  $k^-$ , so we integrate one of them out from  $\phi_B(k^+, k^-, \mathbf{k}_\perp)$ .

For the light-cone wave functions of the  $B$  meson, we use

$$\Phi_{B,\alpha\beta}(x, b) = \frac{i}{\sqrt{2N_c}}[\not{P}_B\gamma_5 + m_B\gamma_5]_{\alpha\beta}\phi_B(x, b), \quad (7)$$

where  $x$  is the momentum fraction of the light quark in  $B$  meson and  $b = |\mathbf{b}|$ , which is the conjugate space coordinate of  $\mathbf{k}_\perp$ . In this paper, we use the following model for  $\phi_B(x, b)$ :

$$\phi_B(x, b) = N_B x^2(1-x)^2 \exp\left[-\frac{m_B^2 x^2}{2\omega_b^2} - \frac{1}{2}(\omega_b b)^2\right]. \quad (8)$$

The normalization factor  $N_B$  is determined by normalization condition.

Decay constant of a scalar glueball state is defined as:

$$\langle G(P)|F^{\mu\rho}F^\nu{}_\rho|0\rangle = f_1 m_{f_0}^2 g^{\mu\nu} + f_s P^\mu P^\nu, \quad (9)$$

where  $F_{\mu\nu}$  is the gluon field strength tensor.  $f_s$  is determined as  $f_s = (100 \sim 130)$  MeV [15]. When the two gluons are separated in coordinate space, the nonperturbative matrix elements are parameterized in terms of the light cone distribution amplitudes (LCDAs). According to the conformal symmetry, the fundamental field with definite twist is the component of the gluon field strength tensor [16]. The component  $F^{\perp\perp}$  is twist-1,  $F^{\perp\perp}$  and  $F^{+-}$  are twist-2 while  $F^{-\perp}$  is twist-3. In the following, we only consider the leading twist light-cone distribution amplitudes of the glueball state:

$$\langle G(P)|F^{a,+\mu}(z^-)F^{b,+\nu}(0)|0\rangle = \int_0^1 dx e^{ixz^-P^+} P^{+2} \frac{f_s \delta^{ab}}{2(N_c^2 - 1)} [g_\perp^{\mu\nu} \phi_G(x)], \quad (10)$$

where  $\mu, \nu$  are the transverse indices. The coordinate  $z$  has been chosen on the light-cone  $z^2 = 0$ . In Eq. (10) we have used the light-cone gauge so that the gauge links between the field strength tensors vanish. The distribution amplitude  $\phi(x)$  can be expanded in terms of the Gegenbauer polynomials:

$$\phi_G(x) = 30x^2(1-x)^2 \left[ 1 + \sum_n a_n C_n^{5/2}(2x-1) \right]. \quad (11)$$

In the  $A^+ = 0$  gauge, the light cone distribution amplitude is reformulated as:

$$\langle G(P)|A^{a\mu}(z^-)A^{b\nu}(0)|0\rangle = - \int_0^1 dx e^{ixz^-P^+} \frac{f_s \delta^{ab}}{2(N_c^2 - 1)} \left[ g_\perp^{\mu\nu} \frac{\phi_G(x)}{x(1-x)} \right], \quad (12)$$

where only the transverse gluon contributes at the leading twist.

Before presenting the formulas for the transition form factors, we will briefly comment on the transverse distribution of the wave functions. The basic idea of the PQCD approach is that it takes into account the transverse momentum of the valence quarks in hadrons which kills the endpoint singularity. The form factor is expressed as a convolution of the wave functions and a hard kernel. Resummation of the double logarithm due to higher order corrections results in the Sudakov factor. Strictly speaking the transverse distribution in all wave functions should be taken into account in the PQCD approach. One of the most acceptable candidates would be the exponential wave function or improved exponential form like the Gaussian one for the  $B$  meson given in Eq. (8). The common feature of these distributions is that the contribution from the large  $b$  region is exponentially suppressed. Meanwhile the Sudakov factor can also suppress the contribution from the large  $b$  region as shown in Fig. 2 in the first paper of Ref. [9]. This suppression effect also depends on the longitudinal momentum. Since the momentum of the quark and antiquark in a light meson is large, contributions from the large  $b$  region are strongly suppressed by the Sudakov factor. As a consequence the role of the transverse distribution in the wave function for the final mesons has already been fulfilled and it can be neglected in the PQCD approach. On the contrary, the Sudakov suppression for the  $B$  meson is not so manifest that the transverse distribution is required. The commonly-used form in the PQCD approach is the one given in Eq. (8) which will be adopted in this work.

The form factors in the PQCD approach are obtained by evaluating the three diagrams in Fig. 1. They can be expressed as the convolution over the longitudinal momentum fraction and the transverse space coordinates:

$$F_1(q^2) = 4 \frac{f_s \sqrt{2N_c}}{N_c^2 - 1} \pi C_F m_B^2 \int_0^1 dx_1 dx_2 \int_0^\infty b_1 db_1 \phi_B(x_1, b_1) \frac{\phi_G(x_2)}{x_2(1-x_2)} \\ \times \left\{ \int_0^\infty b_2 db_2 \{ x_1 [\rho + (1-\rho)x_2] E_a(t_a) h_a + \rho x_2 E_c(t_c) h_c \} + \rho x_2 (1-x_2) E_b(t_b) h_b \right\}, \quad (13)$$

$$F_0(q^2) = 4 \frac{f_s \sqrt{2N_c}}{N_c^2 - 1} \pi C_F m_B^2 \int_0^1 dx_1 dx_2 \int_0^\infty b_1 db_1 \phi_B(x_1, b_1) \frac{\phi_G(x_2)}{x_2(1-x_2)} \\ \times \left\{ \int_0^\infty b_2 db_2 \{ x_1 \rho [2 - \rho + (\rho - 1)x_2] E_a(t_a) h_a + \rho(2 - \rho)x_2 E_c(t_c) h_c \} \right. \\ \left. + \rho^2 x_2 (1-x_2) E_b(t_b) h_b \right\}, \quad (14)$$

$$F_T(q^2) = 4 \frac{(m_B + m_S) f_s \sqrt{2N_c}}{N_c^2 - 1} \pi C_F m_B \int_0^1 dx_1 dx_2 \int_0^\infty b_1 db_1 \phi_B(x_1, b_1) \frac{\phi_G(x_2)}{x_2(1-x_2)} \\ \times \left\{ \int_0^\infty b_2 db_2 \{ x_1 x_2 E_a(t_a) h_a + x_1 (1-x_2) E_c(t_c) h_c \} - x_1 E_b(t_b) h_b \right\}, \quad (15)$$

where  $C_F = 4/3$  and  $N_c = 3$  are color factors.  $E_i, h_i$  are hard functions determined through the propagators in the three diagrams, which are collected in the appendix. Through fitting the results in the hard-scattering region  $0 < q^2 < 10 \text{ GeV}^2$ , we extrapolate them with the dipole model parametrization

$$F_i(q^2) = \frac{F_i(0)}{1 - a(q^2/m_B^2) + b(q^2/m_B^2)^2}, \quad (16)$$

where  $i = 1, 0, T$  and  $a, b$  are parameters to be determined in the fitting procedure.

In the numerical calculation, we adopt  $\omega_B = (0.40 \pm 0.05) \text{ GeV}$  and  $f_B = (0.19 \pm 0.02) \text{ GeV}$  for  $B$  mesons [8]. For the  $B_s$  meson, we use  $\omega_{B_s} = (0.50 \pm 0.05) \text{ GeV}$  and  $f_{B_s} = (0.23 \pm 0.02) \text{ GeV}$  [17]. The decay constant of the scalar glueball is used as  $f_s = 0.13 \text{ GeV}$  [15], but so far there is no theoretical study on the LCDAs of the glueball. The simplest choice is to use the asymptotic form. To roughly estimate the uncertainty from the higher Gegenbauer moment, we will also try the Gegenbauer moment  $a_2 = 0.2$ . The results in table I show that the form factors are sensitive to the Gegenbauer moment  $a_2$ , which will provide relatively important uncertainties to our results. The mass of the glueball is taken as  $m_G = 1.5 \text{ GeV}$ . In the PQCD approach, the  $B$ -to-glueball transition form factors are not very sensitive to this mass.

TABLE I: Distinct contributions to  $B \rightarrow G$  form factors at  $q^2 = 0$ : the index (a,b,c) denotes the contribution from the diagram (a,b,c) in Fig. 1, respectively. Except the results in the last column where  $a_2 = 0$  is used, all other results are obtained with  $a_2 = 0.2$ .

	$a$	$b$	$c$	total	asymptotic
$B \rightarrow G \quad F_1 = F_0$	0.042	0.012	0.001	0.055	0.043
$F_T$	0.035	-0.011	0.001	0.025	0.017
$B_s \rightarrow G \quad F_1 = F_0$	0.038	0.011	0.002	0.051	0.039
$F_T$	0.032	-0.012	0.001	0.020	0.014

TABLE II:  $B \rightarrow G$  and  $B_s \rightarrow G$  form factor with the dipole parametrization. Results in the "asymptotic" ("total") rows correspond to the Gegenbauer moment  $a_2 = 0$  ( $a_2 = 0.2$ ).

	$F_0(0) = F_1(0)$	$F_T(0)$	$a(F_1)$	$b(F_1)$	$a(F_0)$	$b(F_0)$	$a(F_T)$	$b(F_T)$
$B \rightarrow G$ asymptotic	$0.043^{+0.008+0.004}_{-0.007-0.004}$	$0.017^{+0.004+0.001}_{-0.004-0.001}$	$1.22^{+0.00}_{-0.02}$	$0.15^{+0.00}_{-0.02}$	$0.86^{+0.01}_{-0.02}$	$0.06^{+0.02}_{-0.03}$	$1.69^{+0.01}_{-0.03}$	$0.69^{+0.01}_{-0.06}$
$B \rightarrow G$ total	$0.055^{+0.011+0.005}_{-0.009-0.004}$	$0.025^{+0.006+0.002}_{-0.005-0.002}$	$1.24^{+0.01}_{-0.02}$	$0.17^{+0.01}_{-0.02}$	$0.81^{+0.00}_{-0.02}$	$0.03^{+0.01}_{-0.04}$	$1.62^{+0.01}_{-0.04}$	$0.62^{+0.02}_{-0.08}$
$B_s \rightarrow G$ asymptotic	$0.039^{+0.006+0.004}_{-0.005-0.003}$	$0.014^{+0.003+0.001}_{-0.003-0.001}$	$1.20^{+0.01}_{-0.01}$	$0.13^{+0.02}_{-0.01}$	$0.84^{+0.02}_{-0.01}$	$0.04^{+0.03}_{-0.00}$	$1.64^{+0.02}_{-0.02}$	$0.63^{+0.05}_{-0.02}$
$B_s \rightarrow G$ total	$0.051^{+0.008+0.005}_{-0.007-0.004}$	$0.020^{+0.005+0.002}_{-0.004-0.002}$	$1.22^{+0.01}_{-0.01}$	$0.15^{+0.02}_{-0.01}$	$0.79^{+0.02}_{-0.01}$	$0.01^{+0.03}_{-0.01}$	$1.57^{+0.02}_{-0.02}$	$0.54^{+0.05}_{-0.01}$

The distinct contributions from the three diagrams are collected in table I. Among them, the largest contribution is from the first diagram, while the third one is smallest. This is in agreement with the power counting rule given in Sec. II. Although the third diagram can be neglected compared with other potential contributions like the higher order corrections and higher power corrections, this diagram is taken into account since it has the same order in  $\alpha_s$  with the other diagrams. Compared with the gluonic contributions to the  $B \rightarrow \eta$  form factors in Ref. [7], our results are much larger. For the pseudoscalar meson  $\eta$  and  $\eta'$ , the gluonic LCDAs are normalized to 0, thus only higher Gegenbauer moments contribute. The Gegenbauer moment used for the gluonic content of  $\eta$  and  $\eta'$  is very small  $B_2 = \frac{2.1}{30} \sim \frac{7.1}{30}$ . Moreover, we have taken into account the second diagram, which also makes the form factors larger.

In the following, we will comment on the magnitude of  $B$ -to-gluon form factors and compare with other transition form factors. In the PQCD approach, one ingredient for the form factor is the matrix element of the gluon fields and the quark fields. These matrix elements differ with the LCDAs by some constants which can be explicitly given in the definition of the LCDAs. For the gluon state the matrix element associated with the asymptotic twist-2 LCDA defined in Eq. (12) can be rewritten as

$$\frac{1}{2(N_c^2 - 1)} \frac{\phi_G(x)}{x(1-x)} = \frac{30x(1-x)}{2(N_c^2 - 1)},$$

where we have substituted the asymptotic form for the LCDA  $\phi_G(x)$ . Similarly, the matrix element defined by the

TABLE III:  $B \rightarrow f_0(1370)$  and  $B_s \rightarrow f_0(1500)$  form factors in two scenarios (denoted by S1 and S2) with the dipole parametrization, where  $f_0(1370)$  is assigned as  $\bar{n}n$  and  $f_0(1500)$  is identified as  $\bar{s}s$ .

	$F_0(0)$	$F_T(0)$	$a(F_1)$	$b(F_1)$	$a(F_0)$	$b(F_0)$	$a(F_T)$	$b(F_T)$
$B \rightarrow f_0$ S1	$-0.30^{+0.08}_{-0.09}$	$-0.39^{+0.10}_{-0.11}$	$1.63^{+0.09}_{-0.05}$	$0.53^{+0.14}_{-0.08}$	$0.70^{+0.07}_{-0.02}$	$-0.24^{+0.15}_{-0.05}$	$1.60^{+0.06}_{-0.04}$	$0.50^{+0.08}_{-0.05}$
$B \rightarrow f_0$ S2	$0.63^{+0.23}_{-0.14}$	$0.76^{+0.37}_{-0.17}$	$1.60^{+0.15}_{-0.05}$	$0.53^{+0.18}_{-0.09}$	$0.70^{+0.05}_{-0.11}$	$-0.14^{+0.02}_{-0.09}$	$1.63^{+0.07}_{-0.05}$	$0.57^{+0.07}_{-0.07}$
$B_s \rightarrow f_0$ S1	$-0.26^{+0.09}_{-0.08}$	$-0.34^{+0.10}_{-0.10}$	$0.72^{+0.14}_{-0.08}$	$-0.20^{+0.10}_{-0.10}$	$1.61^{+0.13}_{-0.03}$	$0.48^{+0.27}_{-0.02}$	$1.60^{+0.06}_{-0.04}$	$0.48^{+0.09}_{-0.04}$
$B_s \rightarrow f_0$ S2	$0.60^{+0.20}_{-0.12}$	$0.82^{+0.30}_{-0.16}$	$0.65^{+0.04}_{-0.10}$	$-0.22^{+0.07}_{-0.02}$	$1.76^{+0.13}_{-0.08}$	$0.71^{+0.20}_{-0.08}$	$1.71^{+0.04}_{-0.07}$	$0.66^{+0.06}_{-0.10}$

quark fields for a pseudoscalar meson is given by

$$\frac{\phi_P(x)}{4N_c} = \frac{6x(1-x)}{4N_c},$$

where the asymptotic form for the twist-2 LCDA  $\phi_P(x)$  is used:  $\phi_P(x) = 6x(1-x)$  [16]. The prefactor for the glueball is almost 4 times larger than that for a pseudoscalar meson. Despite it, the  $B$ -to-glueball form factors are smaller than the  $B \rightarrow \pi$  form factors. Compared with our previous studies [18, 19] on the transition form factors of  $B$  meson decays into ordinary scalar mesons in Tab. III, the  $B \rightarrow G$  form factors are smaller by a factor of 6–10. One reason is that the decay constant for glueball is smaller than the scalar decay constant for the quark content. For example, the scalar decay constant for  $a_0(1450)$  is  $-0.28 \pm 0.03$  or  $0.46 \pm 0.05$  [20]. There exist some other reasons. In the transition form factors for the quark content, the small momentum fraction  $x_1$  in the numerator of the first diagram in Fig. 1 is replaced by the factor accompanied with the twist-3 LCDA:  $2r_S = \frac{2m_S}{m_B}$ . Although all of these two terms have the same power, the transition for the quark content is much larger than that for the gluon component since  $2r_S \gg \langle x_1 \rangle$  ( $\langle x_1 \rangle$  is the typical value of  $x_1$ ). For the second diagram, the longitudinal momentum of the quark propagators are given as:  $x_2 \bar{x}_2 x_1$ , while the corresponding one that appears in the quark transition form factor is  $\bar{x}_2^2 x_1$ . In the latter case, the region with small values of  $\bar{x}_2$  will give relatively large contributions although the endpoint singularities are removed by the transverse momentum and the threshold resummation. In the former transition, the form factor is directly reduced by the propagators and the contributions from the small momentum fraction region are small. The third diagram is power suppressed as we have discussed. Thus the total form factors are smaller than those for quark contents.

Results for the  $B \rightarrow G$  form factors, together with the  $q^2$ -dependent parameters in Eq. (16), are collected in Tab. II. The uncertainties are from the input parameters: (i) the  $B$  meson decay constant and the shape parameter ( $\omega_B, \omega_{B_s}$ ) in the wave functions; (ii) the factorization scale from  $0.75t$  to  $1.25t$  (not changing the transverse part  $1/b_i$ ):

$$\begin{aligned} \max[0.75\sqrt{\rho x_1} m_B, 1/b_1, 1/b_2] < t_a < \max[1.25\sqrt{\rho x_1} m_B, 1/b_1, 1/b_2], \\ \max[0.75\sqrt{\rho x_2} m_B, \sqrt{\rho \bar{x}_2 x_1} m_B, 1/b_1] < t_b < \max[1.25\sqrt{\rho x_2} m_B, \sqrt{\rho \bar{x}_2 x_1} m_B, 1/b_1], \\ \max[0.75\sqrt{\rho} m_B, 1/b_1, 1/b_2] < t_c < \max[1.25\sqrt{\rho} m_B, 1/b_1, 1/b_2], \end{aligned}$$

and the hadronic scale  $\Lambda_{\text{QCD}} = (0.25 \pm 0.05)$  GeV. The  $q^2$ -dependence of the  $B \rightarrow G$  form factors, together with the form factors for ordinary scalar mesons, are given in Fig. 2. The dashed (black) and solid (red) lines denote the form factors for ordinary mesons in scenario I and scenario II, while the dash-dotted (blue) lines denote the  $B \rightarrow G$  form factors.

Although form factors of  $B$  decays into scalar glueballs are smaller than those for the quark content, one can not neglect the gluon content in the case of mixing for scalar mesons. There is a nontrivial factor  $1/\sqrt{2}$  in form factors for the quark content in  $B$  meson decays. This factor will make the glue component in a scalar meson more important. Compared with the ordinary  $B \rightarrow S$  form factors, the PQCD calculation of the  $B \rightarrow G$  form factors is expected to be more reliable. In the ordinary  $B \rightarrow S$  form factors, the perturbative hard-scattering diagrams contain the endpoint singularity in the collinear factorization. Although the inclusion of the transverse momentum can resolve this problem, the results would still be sensitive to the treatment of the endpoint region. In the PQCD approach resummation of the double logarithms results in the Sudakov factor which will suppress contributions from the nonperturbative region (large  $b$  region). This will improve the convergence of the perturbation theory. These Sudakov effects in  $B \rightarrow \pi$  transition have also been investigated in Ref. [21] with a different conclusion (see Ref. [22] for the response). On the contrary, the situation is different in the  $B$ -to-glueball transition which is free from the endpoint singularity. The results are more stable than the  $B \rightarrow S$  form factors.



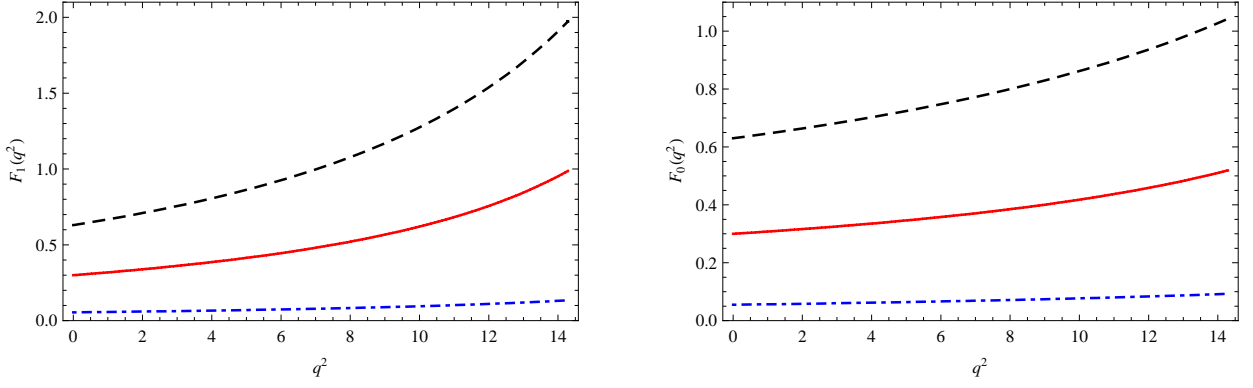


FIG. 2: The  $q^2$ -dependence of  $B \rightarrow S$  form factors  $|F_1(q^2)|$  and  $|F_0(q^2)|$ , where the dashed (black) and solid (red) lines denote the form factors for ordinary mesons in scenario I and scenario II, while the dash-dotted (blue) lines denote the  $B \rightarrow G$  form factors.

#### IV. PHENOMENOLOGICAL APPLICATIONS

##### A. Semileptonic $B \rightarrow Gl\bar{\nu}$ and $B \rightarrow Gl^+l^-$ decays

Integrating out the highly off-shell intermediate degrees of freedom, the effective Hamiltonian for  $b \rightarrow ul\bar{\nu}_l$  transition is given by [23]

$$\mathcal{H}_{\text{eff}}(b \rightarrow ul\bar{\nu}_l) = \frac{G_F}{\sqrt{2}} V_{ub} \bar{u} \gamma_\mu (1 - \gamma_5) b \bar{l} \gamma^\mu (1 - \gamma_5) \nu_l. \quad (17)$$

while the effective Hamiltonian responsible for the  $b \rightarrow Dl^+l^-$  ( $D = d, s$ ) transition is

$$\mathcal{H}_{\text{eff}} = -\frac{G_F}{\sqrt{2}} V_{tb} V_{tD}^* \sum_{i=1}^{10} C_i(\mu) O_i(\mu), \quad (18)$$

where  $V_{ub}, V_{tb}$  and  $V_{tD}$  ( $D = d, s$ ) are the Cabibbo-Kobayashi-Maskawa (CKM) matrix elements.  $C_i(\mu)$  are the Wilson coefficients and the local operators  $O_i(\mu)$  are given by

$$\begin{aligned} O_1 &= (\bar{D}_\alpha c_\alpha)_{V-A} (\bar{c}_\beta b_\beta)_{V-A}, & O_2 &= (\bar{D}_\alpha c_\beta)_{V-A} (\bar{c}_\beta b_\alpha)_{V-A}, \\ O_3 &= (\bar{D}_\alpha b_\alpha)_{V-A} \sum_q (\bar{q}_\beta q_\beta)_{V-A}, & O_4 &= (\bar{D}_\alpha b_\beta)_{V-A} \sum_q (\bar{q}_\beta q_\alpha)_{V-A}, \\ O_5 &= (\bar{D}_\alpha b_\alpha)_{V-A} \sum_q (\bar{q}_\beta q_\beta)_{V+A}, & O_6 &= (\bar{D}_\alpha b_\beta)_{V-A} \sum_q (\bar{q}_\beta q_\alpha)_{V+A}, \\ O_7 &= \frac{em_b}{8\pi^2} \bar{D} \sigma^{\mu\nu} (1 + \gamma_5) b F_{\mu\nu} + \frac{em_D}{8\pi^2} \bar{D} \sigma^{\mu\nu} (1 - \gamma_5) b F_{\mu\nu}, \\ O_9 &= \frac{\alpha_{\text{em}}}{2\pi} (\bar{l} \gamma_\mu l) (\bar{D} \gamma^\mu (1 - \gamma_5) b), & O_{10} &= \frac{\alpha_{\text{em}}}{2\pi} (\bar{l} \gamma_\mu \gamma_5 l) (\bar{D} Z \gamma^\mu (1 - \gamma_5) b), \end{aligned} \quad (19)$$

where  $(\bar{q}_1 q_2)_{V-A} (\bar{q}_3 q_4)_{V-A} \equiv (\bar{q}_1 \gamma^\mu (1 - \gamma_5) q_2) (\bar{q}_3 \gamma_\mu (1 - \gamma_5) q_4)$ , and  $(\bar{q}_1 q_2)_{V-A} (\bar{q}_3 q_4)_{V+A} \equiv (\bar{q}_1 \gamma^\mu (1 - \gamma_5) q_2) (\bar{q}_3 \gamma_\mu (1 + \gamma_5) q_4)$ .  $\alpha, \beta$  are the color indices for the quark field.  $\alpha_{\text{em}} = 1/137$  is the fine structure constant. The amplitude for  $b \rightarrow sl^+l^-$  transition can be decomposed as

$$\begin{aligned} \mathcal{A}(b \rightarrow sl^+l^-) &= \frac{G_F}{2\sqrt{2}} \frac{\alpha_{\text{em}}}{\pi} V_{tb} V_{ts}^* \left\{ C_9^{\text{eff}}(q^2) [\bar{s} \gamma_\mu (1 - \gamma_5) b] [\bar{l} \gamma^\mu l] + C_{10} [\bar{s} \gamma_\mu (1 - \gamma_5) b] [\bar{l} \gamma^\mu \gamma_5 l] \right. \\ &\quad \left. - 2m_b C_7^{\text{eff}} [\bar{s} i \sigma_{\mu\nu} \frac{q^\nu}{q^2} (1 + \gamma_5) b] [\bar{l} \gamma^\mu l] - 2m_s C_7^{\text{eff}} [\bar{s} i \sigma_{\mu\nu} \frac{q^\nu}{q^2} (1 - \gamma_5) b] [\bar{l} \gamma^\mu l] \right\}, \end{aligned} \quad (20)$$



TABLE IV: The values of Wilson coefficients  $C_i(m_b)$  in the leading logarithmic approximation, with  $m_W = 80.4\text{GeV}$ ,  $\mu = m_{b,\text{pole}}$  [23].

$C_1$	$C_2$	$C_3$	$C_4$	$C_5$	$C_6$	$C_7^{\text{eff}}$	$C_9$	$C_{10}$
1.107	-0.248	-0.011	-0.026	-0.007	-0.031	-0.313	4.344	-4.669

with  $m_b$  as the  $b$  quark mass in the  $\overline{\text{MS}}$  scheme and we will use  $m_b = 4.8\text{ GeV}$ .  $C_7^{\text{eff}} = C_7 - C_5/3 - C_6$  and  $C_9^{\text{eff}}$  contains both the long-distance and short-distance contributions, which is given by

$$C_9^{\text{eff}}(q^2) = C_9(\mu) + Y_{\text{pert}}(\hat{s}) + Y_{\text{LD}}(q^2). \quad (21)$$

with  $\hat{s} = q^2/m_B^2$ .  $Y_{\text{pert}}$  represents the perturbative contributions, and  $Y_{\text{LD}}$  is the long-distance part. Since the long-distance contribution can be separated on the experimental side, we will neglect it. The short-distance corrections  $Y_{\text{pert}}$  is given by [24]

$$Y_{\text{pert}}(\hat{s}) = h(\hat{m}_c, \hat{s})C_0 - \frac{1}{2}h(1, \hat{s})(4C_3 + 4C_4 + 3C_5 + C_6) - \frac{1}{2}h(0, \hat{s})(C_3 + 3C_4) + \frac{2}{9}(3C_3 + C_4 + 3C_5 + C_6), \quad (22)$$

with  $C_0 = C_1 + 3C_2 + 3C_3 + C_4 + 3C_5 + C_6$  and  $\hat{m}_c = m_c/m_b$  with  $m_c = 1.27\text{ GeV}$  [25]. The relevant Wilson coefficients, listed in table IV, are given up to the leading logarithmic accuracy [23].

Lepton decay amplitudes can be directly calculated using the perturbation theory. The unknown amplitude is the matrix elements of quark operators which have been parameterized as the form factors. The partial decay width is given by

$$\frac{d\Gamma(B \rightarrow Gl\bar{\nu})}{dq^2} = \frac{\sqrt{\lambda}G_F^2|V_{ub}|^2}{384\pi^3m_B^3q^2} \left(\frac{q^2 - m_l^2}{q^2}\right)^2 \left[ (m_l^2 + 2q^2)\lambda F_1^2(q^2) + 3m_l^2(m_B^2 - m_S^2)^2 F_0^2(q^2) \right], \quad (23)$$

where  $\lambda = (m_B^2 - q^2 - m_G^2)^2 - 4m_G^2q^2$  and  $m_l$  is the lepton mass. Integrating out the momentum transfer square  $q^2$ , we obtain branching ratios of  $B \rightarrow Gl\bar{\nu}$  ( $l = e, \mu$ ) and  $B \rightarrow G\tau\bar{\nu}_\tau$

$$\mathcal{B}(B \rightarrow Gl\bar{\nu}) = (0.18_{-0.06}^{+0.08+0.03+0.02} [0.11_{-0.03-0.02-0.01}^{+0.05+0.02+0.01}]) \times 10^{-5}, \quad (24)$$

$$\mathcal{B}(B \rightarrow G\tau\bar{\nu}_\tau) = (0.08_{-0.03-0.01-0.01}^{+0.03+0.01+0.01} [0.05_{-0.02-0.01-0.00}^{+0.02+0.01+0.00}]) \times 10^{-5}, \quad (25)$$

where results in the square brackets and out of the square brackets are evaluated using the asymptotic form and the form with  $a_2 = 0.2$ , respectively. In the evaluation of semileptonic  $B$  decays we have adopted the dipole form for the form factors given in Eq. (16), where the parameters are obtained through fitting the large recoil region. Uncertainties are from three different kinds of inputs: (i) the  $B$  meson decay constant and the shape parameter ( $\omega_B, \omega_{B_s}$ ), (ii) the hadronic scale  $\Lambda_{\text{QCD}}$ , the factorization scale  $t$ , (iii) the CKM matrix element  $|V_{ub}| = (3.51_{-0.16}^{+0.14}) \times 10^{-3}$  [26]. Compared with the recently measured result of  $B \rightarrow \eta l\bar{\nu}$  decay [27]

$$\mathcal{B}(B^- \rightarrow \eta l^- \bar{\nu}) = (3.1 \pm 0.6 \pm 0.8) \times 10^{-5}, \quad (26)$$

we can see that  $B \rightarrow Gl\bar{\nu}$  ( $l = e, \mu$ ) have smaller branching ratios by one order. The main decay channel of a scalar glueball could be  $\pi\pi$  or  $K\bar{K}$  while the  $\eta$  meson is reconstructed by three pions or two photons. Thus a scalar glueball is easier to detect than the isoscalar meson  $\eta$ , and the  $B \rightarrow Gl\bar{\nu}$  decays may be observed in the future.

The partial decay width of semileptonic  $B_{d,s} \rightarrow Gl^+l^-$  decays is given as

$$\begin{aligned} \frac{d\Gamma(B_{d,s} \rightarrow Gl^+l^-)}{dq^2} &= \sqrt{\frac{q^2 - 4m_l^2}{q^2}} \frac{G_F^2 \alpha_{\text{em}}^2 \sqrt{\lambda}}{1024m_B^3 \pi^5} \times |V_{tb}V_{tD}|^2 \\ &\times \left[ \frac{4}{3} \lambda \left| \frac{C_9^{\text{eff}}}{2} F_1(q^2) + \frac{C_{10}}{2} F_1(q^2) \sqrt{\frac{q^2 - 4m_l^2}{q^2}} + (C_{7L} - C_{7R}) \frac{m_b F_T(q^2)}{m_B + m_P} \right|^2 \right. \\ &+ \frac{4}{3} \lambda \left| \frac{C_9^{\text{eff}}}{2} F_1(q^2) - \frac{C_{10}}{2} F_1(q^2) \sqrt{\frac{q^2 - 4m_l^2}{q^2}} + (C_{7L} - C_{7R}) \frac{m_b F_T(q^2)}{(m_B + m_P)} \right|^2 \\ &\left. + \frac{4\lambda m_l^2}{3q^2} \left| C_9^{\text{eff}} F_1(q^2) + (C_{7L} - C_{7R}) \frac{2m_b F_T(q^2)}{(m_B + m_P)} \right|^2 + \frac{4m_l^2}{q^2} |C_{10}(m_B^2 - m_P^2) F_0(q^2)|^2 \right], \quad (27) \end{aligned}$$

where  $D = d, s$  for  $\bar{B}^0 \rightarrow Gl^+l^-$  and  $\bar{B}_s^0 \rightarrow Gl^+l^-$  decays.  $m_l$  denotes the lepton's mass and  $C_{7L} = C_7^{\text{eff}}$ ,  $C_{7R} = \frac{m_{s,d}}{m_b} C_7^{\text{eff}} \sim 0$ . Branching fractions of  $B \rightarrow Gl^+l^-$  and  $B_s \rightarrow Gl^+l^-$  decays are predicted as

$$\mathcal{B}(B \rightarrow Gl^+l^-) = (0.27_{-0.09-0.04}^{+0.12+0.05} [0.18_{-0.05-0.03}^{+0.07+0.03}]) \times 10^{-9}, \quad (28)$$

$$\mathcal{B}(B \rightarrow G\tau^+\tau^-) = (0.5_{-0.2-0.1}^{+0.2+0.1} [0.3_{-0.1-0.1}^{+0.1+0.1}]) \times 10^{-11}, \quad (29)$$

$$\mathcal{B}(B_s \rightarrow Gl^+l^-) = (0.6_{-0.2-0.1}^{+0.2+0.1} [0.4_{-0.1-0.1}^{+0.1+0.1}]) \times 10^{-8}, \quad (30)$$

$$\mathcal{B}(B_s \rightarrow G\tau^+\tau^-) = (0.18_{-0.05-0.03}^{+0.07+0.04} [0.12_{-0.03-0.02}^{+0.04+0.02}]) \times 10^{-9}. \quad (31)$$

Uncertainties are from two different kinds of inputs in the PQCD approach: (i) the  $B$  meson decay constant and the shape parameter  $(\omega_B, \omega_{B_s})$ , (ii) the hadronic scale  $\Lambda_{\text{QCD}}$ , the factorization scale  $t$ . The CKM matrix element  $V_{td} = (8.59_{-0.29}^{+0.28}) \times 10^{-3}$ ,  $V_{ts} = -(40.42_{-0.37}^{+1.18}) \times 10^{-3}$  and  $V_{tb} = 0.999146_{-0.000016}^{+0.000048}$  [26] will not give large uncertainties. The  $B \rightarrow Gl^+l^-$  has tiny branching fractions, which can not be observed on the present  $B$  factories, especially the  $B \rightarrow G\tau^+\tau^-$  with a very small phase space. But the  $B_s \rightarrow Gl^+l^-$  decay channel may be observed on the future experiment, since it has a sizable branching fraction.

The physical scalar meson is probably a mixture of glueball and ordinary states, so the predicted branching ratios in eq.(24,25,28-31) will be smaller for physical scalar meson, according to the gluon component of each scalar meson. The experimental accessibility will still be large, at least for the scalar mesons with large glue components.

## B. Mixing between scalar mesons

There is not any solid experimental evidence for a pure glueball state up to now. Lattice QCD predicted the mass of a scalar glueball ground state around 1.5-1.8 GeV [1, 2]. At present most of the lattice studies on hadronic correlators are in the quenched approximation by neglecting the fluctuations of the quarks. Due to the lack of dynamical quarks, the binding of quark-antiquark systems must be attributed to the nonperturbative properties of gluons, the unique dynamical degree of freedom in the Lattice QCD. Secondly the simulations are based on the computation of the matrix element of the gluon operators, while the glueball states  $G$  are obtained by smeared gluonic operators since there is no physical glueball state. Nevertheless, despite these ambiguities the Lattice QCD simulations give us a hint that one scalar glueball state might exist around this mass region. It is very likely that the glueball state mixes with the ordinary quark-antiquark state to form several physical mesons.

In the literature, three scalar mesons  $f_0(1370)$ ,  $f_0(1500)$  and  $f_0(1710)$  are usually considered as the potential

candidates. The mixing matrix can be generally set as

$$\begin{pmatrix} f_0(1710) \\ f_0(1500) \\ f_0(1370) \end{pmatrix} = \begin{pmatrix} a_1 & a_2 & a_3 \\ b_1 & b_2 & b_3 \\ c_1 & c_2 & c_3 \end{pmatrix} \begin{pmatrix} G \\ \bar{s}s \\ \bar{n}n \end{pmatrix}. \quad (32)$$

The unitary condition implies that the mixing matrix has only three independent real numbers. A non-zero  $a_1$ ,  $b_1$  or  $c_1$  would be a clear evidence for the existence of a glueball. The semileptonic  $B \rightarrow f_0 l \bar{\nu}$  decays receive contributions from the  $\bar{n}n$  component and glue component but without  $\bar{s}s$  component (at least negligible), while the semileptonic  $B_s \rightarrow f_0 l^+ l^-$  channel only receive contributions from the  $\bar{s}s$  and glue component but without  $\bar{n}n$  component. Thus the experimental measurements for the two channels can give effective constraints to the mixing parameters. For the three kinds of flavor singlet scalar mesons, we have altogether 6 experiments, but only three real parameters in eq.(32) to be fixed. Since the branching fraction of  $B_s \rightarrow f_0 l^+ l^-$  is expected to have the order of  $10^{-8}$  or even smaller, one needs to accumulate a large number of  $B$  decay events, which could be achieved on the future experiments such as the Super B factory.

Taking into account the current available experimental data, the mixing mechanism is still not fixed, for example there are two quite different mixing matrix determined by two group of people. Because the decay width of  $f_0(1500)$  is not compatible with the ordinary  $\bar{q}q$  state, Amsler and Close claimed that  $f_0(1500)$  is primarily a scalar glueball [28]. In the subsequent studies [29], they extracted the mixing matrix through fitting the data of two-body decays of scalar mesons

$$\begin{pmatrix} f_0(1710) \\ f_0(1500) \\ f_0(1370) \end{pmatrix} = \begin{pmatrix} 0.36 & 0.93 & 0.09 \\ -0.84 & 0.35 & -0.41 \\ 0.40 & -0.07 & -0.91 \end{pmatrix} \begin{pmatrix} G \\ \bar{s}s \\ \bar{n}n \end{pmatrix}. \quad (33)$$

Based on the SU(3) assumption for scalar mesons and the quenched Lattice QCD results [2], Cheng et al. [30] reanalyze all existing experimental data and fit the mixing coefficient as

$$\begin{pmatrix} f_0(1710) \\ f_0(1500) \\ f_0(1370) \end{pmatrix} = \begin{pmatrix} 0.93 & 0.17 & 0.32 \\ -0.03 & 0.84 & -0.54 \\ -0.36 & 0.52 & 0.78 \end{pmatrix} \begin{pmatrix} G \\ \bar{s}s \\ \bar{n}n \end{pmatrix}. \quad (34)$$

Here, the  $f_0(1710)$  tends to be a primary glueball. This is very different from the first matrix of mixing coefficients in (33). The scalar meson production rates in  $B$  meson decays can be used to distinguish these assignments, starting with the  $B \rightarrow S$  form factors collected in Tab. II and Tab. III.

- In scenario I, if we use the mixing coefficients in Eq. (33), the production rates of  $f_0(1710)$  and  $f_0(1500)$  in  $B$  decays are much smaller than that of  $f_0(1370)$  but they have large and comparable production rates in  $B_s$  decays; if we use the mixing coefficients in Eq. (34),  $f_0(1710)$  has small production rates in both  $B$  and  $B_s$  decays but the other two mesons have large and comparable production rates in  $B$  and  $B_s$  decays.
- In scenario II, if we use the mixing coefficients in Eq. (33), production rates of  $f_0(1370)$  and  $f_0(1500)$  in  $B$  decays are large and comparable, and  $f_0(1710)$  is copious in  $B_s$  decays; if we use the mixing coefficients in Eq. (34), three mesons have similar production rates in  $B$  decays, and  $f_0(1500)$  is more copious than  $f_0(1370)$  and  $f_0(1710)$  in  $B_s$  decays.

Based on our predictions on form factors in this work and in our previous studies [18, 19], these differences in  $B$  and  $B_s$  decays are helpful to distinguish the two mixing mechanisms. Once the branching fraction of these decays were measured, our calculation can be used to constrain the mixing angle. One more practical method in future would

be to use the  $\chi^2$ -fit method and take the theoretical and experimental uncertainties into account. This requires the future experimental studies.

The main decay channel of a scalar meson would be  $G \rightarrow PP$ , and thus the scalar meson could be reconstructed from  $\pi^+\pi^-$  or  $K^+K^-$ . The scalar meson may also decay into a pair of vectors and thus it could be reconstructed as 4 pions. For the three candidates of glueball states, the reconstruction method is different. If  $f_0(1370)$  is the dominant glueball state, the best candidate is from 4-pion state, since its main decay mode is  $f_0(1370) \rightarrow \rho\rho$  [25]. For  $f_0(1500)$ , the dominant mode is  $f_0(1500) \rightarrow \pi\pi(34.9 \pm 2.3\%)$  and  $f_0(1500) \rightarrow 4\pi(49.5 \pm 3.3\%)$ . As for  $f_0(1710)$ , the dominant decay mode is  $f_0(1710) \rightarrow K\bar{K}$ .

### C. Uncertainty analysis

Besides the uncertainties that we have already given in the above, there exist several other uncertainties, which may affect the extraction of the mixing matrix of scalar mesons.

- Our results depend on the form factors calculated in the perturbative QCD approach, which is based on the  $k_T$  factorization. The application of PQCD approach to many channels involving the s-wave mesons is successful. Phenomenologically, the large annihilations can explain the correct branching ratios and direct CP asymmetries of  $\bar{B}^0 \rightarrow \pi^+\pi^-$  and  $\bar{B}^0 \rightarrow K^-\pi^+$  [31], the polarization problem of  $B \rightarrow \phi K^*$  [32], etc. Up to now, this approach is only at the leading order in  $1/m_B$  expansion, without the next-to-leading order corrections. Since the scalar glueball is not very light, the power corrections proportional to  $m_S/m_B$  may also be important. Moreover although this approach has been proved for the  $B \rightarrow \pi$  form factor [33], there is no proof for the factorization of the  $B$ -to-glueball form factor and this may introduce some potential uncertainties.
- The hadronic inputs give another origin of the uncertainties. The decay constant  $f_s$  of a scalar glueball may introduce sizable uncertainties (roughly 20%). Since there is not any theoretical study on the LCDA of scalar glueball, the higher but unknown Gegenbauer moments in the LCDA may also provide sizable contributions.
- In the presence of mixing, the uncertainties from ordinary scalar mesons also affect the production rates of scalar glueballs sizably. For example in the two different scenarios for scalar mesons, the form factors for the quark states even have different signs, because of the different signs in the decay constants of ordinary scalar mesons [20]. Accordingly, the interference between quark content and gluon content differs in signs in the two scenarios. Moreover, the magnitudes of decay constants could also suffer from large ambiguities. We take the decay constant of  $f_0(980)$  as an example. Based on the two-quark assumption for the  $f_0(980)$  meson, the early study in the QCD sum rule [35] gives

$$\bar{f}_{f_0(980)} = (0.18 \pm 0.015)\text{GeV},$$

while the recent study [20] predicts two sets of values

$$\bar{f}_{f_0(980)} = (0.37 \pm 0.02)\text{GeV}[(0.46 \pm 0.025)\text{GeV}],$$

at the scale  $\mu = 1\text{GeV}$  ( $\mu = 2.1\text{GeV}$ ). The decay constants for the isosinglet mesons near 1.5 GeV may also suffer from similar uncertainties and the interference between different components will be complicated.

These quantities will inevitably affect the production rates of scalar mesons, and the extraction of the mixing matrix will require more precise, both experimental and theoretical, studies. For example, the experimental study on semileptonic  $B \rightarrow a_0(1450)$  decays is helpful to constrain the contributions from the quark content. On the theoretical side uncertainties caused by the hadronic inputs could be reduced in a systematic and comprehensive study on the ordinary scalar meson and the glueball state. This is beyond the scope of this work and will be reported elsewhere.

### D. Comparison with other works

In Ref. [5], the authors investigated the inclusive  $B \rightarrow X_s G$  decay, where the large production rate of  $f_0(1710)$  is viewed as the signal of a scalar glueball. The rate of  $B$  decays into a scalar glueball through gluonic penguin is expected to be sizable, but  $B \rightarrow X_s G$  is an inclusive mode, which is more difficult than exclusive  $B$  meson decays experimentally. The background from the other mesons may also pollute their method. The authors in Ref. [4] used symmetries of the penguin contributions and studied the production rates of a scalar glueball in charmless three-body  $B$  decays. Irrespective of the validity of neglecting contributions from tree operators (with large Wilson coefficients) and the uncertainties from the symmetry breaking effect, much more data on the  $B \rightarrow S$  decays is required to make precise predictions.

In Ref. [6], the author studied the exclusive channel  $B \rightarrow GK(K^*)$  which could be experimentally detected. Since it is a nonleptonic decay, the uncertainties would be larger than those in  $B \rightarrow Gl\bar{\nu}$  and  $B_{d,s} \rightarrow Gl^+l^-$  decays.  $B \rightarrow GK$  is a penguin-dominated process, which is purely induced by the loop effect in the standard model. The relevant Wilson coefficient is small and the result is sensitive to the next-to-leading order correction and/or the potential new physics effect. Hadronic uncertainties are also typically large in nonleptonic decays. Contributions from the  $B \rightarrow G$  transition form factor are neglected in their analysis. The light-cone distribution amplitude is not used in their work, thus the internal structure of a scalar glueball could not completely reflected. It would be interesting to reanalyze this nonleptonic decay channel by combining our prediction on the form factors and the other amplitudes studied in their work.

Compared with the studies in the literature, we can see that albeit the production rates of a glueball state in semileptonic  $B$  decays are not very large, the chosen channels  $B \rightarrow Gl\bar{\nu}$  and  $B_s \rightarrow Gl^+l^-$  are easily measured and rather clean. In inclusive decays  $B \rightarrow X_s G$  decays, it is almost impossible to study the mixing between ordinary scalar mesons and a glueball state.

### E. Some discussions on nonleptonic $B$ decays

Semileptonic  $B$  decays are clean but in  $B \rightarrow f_0 l \bar{\nu}$ , the neutrino is identified as missing energy and the efficiency is limited; while the  $B_s \rightarrow f_0 l^+ l^-$  has a small branching ratio. In these decays, the lepton pair does not carry any SU(3) flavor and the decay amplitudes receive less pollution from the strong interactions. The lepton pair can also be replaced by a charmonium state such as  $J/\psi$  since  $J/\psi$  does not carry any light flavor either.  $B \rightarrow J/\psi f_0$  decays may provide another ideal probe to detect the internal structure of the scalar mesons. In  $B \rightarrow J/\psi f_0$  decay, the  $\bar{s}s$  component will not contribute at the leading order in  $\alpha_s$ . For example, the  $B \rightarrow J/\psi \phi$  decay has been set a very stringent upper limit [34]:  $\mathcal{B}(B \rightarrow J/\psi \phi) < 9.4 \times 10^{-7}$ . Thus  $B \rightarrow J/\psi f_0$  decay can filter out the glueball component and the  $\bar{n}n$  component of a scalar meson. Meanwhile in  $B_s \rightarrow J/\psi f_0$  decay, only the  $\bar{s}s$  and the gluon component contribute. Moreover, the final state mesons in these channels are easy to reconstruct and these channels could have sizable branching fractions. If we use the factorization method, decay amplitudes are given as

$$A(\bar{B}^0 \rightarrow J/\psi f_0) = \frac{G_F}{\sqrt{2}} V_{cb} V_{cd}^* (2\epsilon_{J/\psi}^* \cdot P_B) f_{J/\psi} a_2 F_1^{B \rightarrow f_0}(m_{J/\psi}^2). \quad (35)$$

The Wilson coefficient  $a_2$  can be extracted from the  $B \rightarrow J/\psi K$  decays [25]

$$\mathcal{B}(\bar{B}^0 \rightarrow J/\psi \bar{K}^0) = (8.71 \pm 0.32) \times 10^{-4}. \quad (36)$$

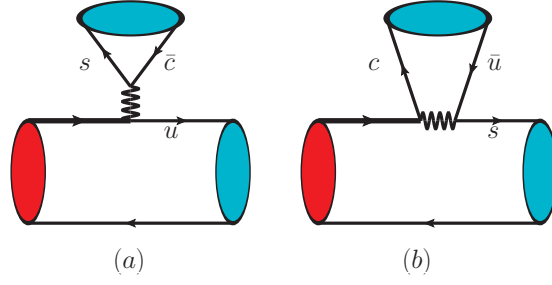


FIG. 3: Feynman diagrams of  $B \rightarrow f_0 D$  and  $B_s \rightarrow f_0 \bar{D}$  decays. These channels suffer large uncertainties.

The branching ratios are roughly predicted as

$$\mathcal{B}(\bar{B}^0 \rightarrow J/\psi f_0(\bar{n}n)) \simeq \begin{cases} (23_{-14}^{+12}) \times 10^{-6} & \text{S1} \\ (10_{-5}^{+7}) \times 10^{-5} & \text{S2} \end{cases}, \quad (37)$$

$$\mathcal{B}(\bar{B}^0 \rightarrow J/\psi G) \simeq (1.5 \pm 0.5) \times 10^{-6}, \quad (38)$$

where we have assumed the same  $q^2$  dependence for all form factors and  $F_1^{B \rightarrow K}(0) = 0.3$ . The uncertainties are from the experimental data for  $\mathcal{B}(B \rightarrow J/\psi K)$  and the  $B \rightarrow S$  form factors at the  $q^2 = 0$  point. For the  $B_s$  decays, the branching ratios are comparable with that of  $B \rightarrow J/\psi K$ :

$$\mathcal{B}(\bar{B}_s \rightarrow J/\psi f_0(\bar{s}s)) \simeq \begin{cases} (6.5_{-4.5}^{+4.0}) \times 10^{-4} & \text{Scenario 1} \\ (3.5_{-1.4}^{+2.3}) \times 10^{-3} & \text{Scenario 2} \end{cases}, \quad (39)$$

$$\mathcal{B}(\bar{B}_s \rightarrow J/\psi G) \simeq (2.4 \pm 1.0) \times 10^{-5}. \quad (40)$$

Such large branching fractions offer a great opportunity to probe structures of scalar mesons. With the available data in the future, the mixing problem between the scalar mesons will be solvable and the glueball component can be projected out in principle.

If the power-suppressed annihilation diagrams are neglected, the charmful decays of  $B$  meson,  $B \rightarrow f_0 D$ , can also be used to constrain the mixing between scalar mesons. For instance in  $B^- \rightarrow D_s^- f_0$ , the  $\bar{n}n$  and gluon component contribute but the  $\bar{s}s$  component does not, while in  $\bar{B}_s \rightarrow D^0 f_0$ , the  $\bar{n}n$  component will not contribute, as shown in Fig. 3. Thus the mixing coefficients can also be determined if these two channels are experimentally measured. It is necessary to point out that this method may suffer from sizable uncertainties of annihilation diagrams [18].

### F. Glueball production in $B_c$ decays

The ordinary light scalar meson is isospin singlet and/or flavor SU(3) singlet, while the glueball is flavor SU(6) singlet. Therefore it is difficult to distinguish them by the light  $u$ ,  $d$  and  $s$  quark coupling. However, the light ordinary scalar meson has negligible  $c\bar{c}$  component, while the glueball have the same coupling to  $c\bar{c}$  as that to the  $u\bar{u}$ ,  $d\bar{d}$  or  $s\bar{s}$ . A clean way to identify a glueball is then through the  $c\bar{c}$  coupling to the glueball.

In  $B$  decays, the initial heavy meson contains a light quark, thus contributions of the gluon component always accompany with the quark content  $\bar{n}n$  or  $\bar{s}s$ . It is not easy to isolate the gluon content. The situation in the doubly-heavy  $B_c$  meson is different: it contains a heavy charm antiquark. The semileptonic  $B_c \rightarrow f_0 l \bar{\nu}$  decays would happen only through Fig. 1(a)(b) and (c) but not through Fig. 1(d) and (e). The observation of this decay channel in the experiments will surely establish the existence of a scalar glueball. Moreover the CKM matrix element in this channel is  $V_{cb}$ , thus the  $B_c \rightarrow f_0 l \bar{\nu}$  will have a sizable branching ratio. This channel will depend on the  $B_c \rightarrow G$  transition

form factor which requires the less-constrained  $B_c$  meson's light-cone distribution amplitude. But even if we assume the form factor of  $B_c \rightarrow G$  is smaller than the  $B_c \rightarrow \eta_c$  form factor by one order, branching ratios of  $B_c \rightarrow Gl\bar{\nu}(l\bar{\nu})$  are suppressed by two orders

$$\mathcal{B}(B_c \rightarrow Gl\bar{\nu}) \sim 1\% \times 0.01 = 10^{-4}, \quad (41)$$

where the branching ratio of  $B_c \rightarrow \eta_c l\bar{\nu}$  has been taken as 1%. Although more quantitative results need the precise  $B_c \rightarrow G$  form factors, which requires the  $B_c$  wave function with large uncertainties, the order of magnitude of branching ratio is convincing. This branching ratio is large enough for the experiments. One only needs to reconstruct the  $f_0$  scalar meson in the final state and also the  $B_c$  meson mass in the intermediate state, so that to make sure that the scalar meson is produced from two gluons. That experiment is achievable even if the  $f_0$  meson is not a pure glueball, but at least has a large portion of it. The disadvantage here is the missing neutrino in detector is hard to be reconstructed in hadronic machines, like LHCb. A future Z factory is an ideal place for this channel to be measured [36].

$B_c \rightarrow f_0\pi^-$  is another potential mode to figure out the gluon content. But in this mode, the  $\bar{n}n$  component also contributes through the annihilation diagrams. The  $b$  and  $\bar{c}$  quark annihilates and the  $d$  and  $\bar{u}$  quark are created. The CKM matrix element  $V_{cb}$  and the Wilson coefficient  $a_1$  are the same with the emission diagram for the  $B_c$ -to-gluon transition. The offshellness of the two internal particles in annihilation diagrams are of the order  $m_{B_c}^2$ . The electroweak vertex is the  $V-A$  type and the decay amplitude is proportional to the light quark mass. Thus the decay amplitudes via annihilation diagram for the  $\bar{n}n$  component are expected to be suppressed. As a result, the  $B_c \rightarrow f_0\pi^-$  also filters out the gluon component of the scalar meson as an approximation.

## V. CONCLUSIONS

In this work, we have investigated the transition form factors of  $B$  meson decays into a scalar glueball state in the PQCD approach. Compared with the form factors for the quark content, we find that form factors for the gluon content have the same power counting in the expansion of  $\Lambda_{\text{QCD}}/m_B$  but they are numerically a little smaller. The pure glueball states can be detected in semileptonic  $B \rightarrow Gl\bar{\nu}$  and  $B_s \rightarrow Gl^+l^-$  in the future, since they have a sizeable branching ratio.

If a scalar meson is a mixture of a glueball and an ordinary meson, we investigate the possibility to extract the mixing mechanism from semileptonic  $B$  decays, such as  $B \rightarrow f_0 l\bar{\nu}$  and  $B_s \rightarrow f_0 l^+ l^-$  decays. The nonleptonic  $B \rightarrow J/\psi f_0$  and  $B_s \rightarrow J/\psi f_0$  decays are also analyzed. To be specific, we discussed the production rates of scalar mesons under two different mixing mechanisms, and we find that the differences in  $B$  and  $B_s$  decays are helpful to distinguish the two mixing mechanisms. To avoid the interference between the quark and the gluon component, we find that the  $B_c \rightarrow f_0 l\bar{\nu}$  and  $B_c \rightarrow f_0\pi^-$  will project out the gluon component of a scalar meson cleanly. Our results can be generalized to the other glueballs.

## Acknowledgement

This work is partly supported by National Natural Science Foundation of China under the Grant No. 10735080, 10625525, and 10847161 and Natural Science Foundation of Zhejiang Province of China, Grant No. Y606252. We would like to acknowledge Prof. Hsiang-nan Li for useful discussions.



### Appendix A: hard kernels

Hard scales and functions in the  $B \rightarrow G$  form factors are defined by:

$$t_a = \max[\sqrt{\rho x_1} m_B, 1/b_1, 1/b_2], \quad (\text{A1})$$

$$t_b = \max[\sqrt{\rho x_2} m_B, \sqrt{\rho \bar{x}_2 x_1} m_B, 1/b_1], \quad (\text{A2})$$

$$t_c = \max[\sqrt{\rho} m_B, 1/b_1, 1/b_2], \quad (\text{A3})$$

$$E_a(t_a) h_a = \alpha_s(t_a) \exp[-S_B(t_a) - S_G(t_a)] [\theta(b_1 - b_2) I_0(\sqrt{\rho x_1} m_B b_2) K_0(\sqrt{\rho x_1} m_B b_1) \quad (\text{A4})$$

$$+ \theta(b_2 - b_1) I_0(\sqrt{\rho x_1} m_B b_1) K_0(\sqrt{\rho x_1} m_B b_2)] K_0(\sqrt{\rho \bar{x}_2 x_1} m_B b_2), \quad (\text{A5})$$

$$E_b(t_b) h_b = \alpha_s(t_b) \exp[-S_B(t_b) - S_G(t_b)] \int_0^1 dz \frac{b_1}{2\sqrt{Z_1}} K_1(\sqrt{Z_1} b_1), \quad (\text{A6})$$

$$E_c(t_c) h_c = (E_a(t_a) h_a)|_{x_1 \rightarrow 1, \bar{x}_2 \rightarrow x_2}, \quad (\text{A7})$$

where  $Z_1$  is defined as

$$Z_1 = \rho x_2 m_B^2 z + \rho \bar{x}_2 x_1 m_B^2 (1 - z). \quad (\text{A8})$$

The Sudakov factors are given by:

$$S_B(t) = s\left(x_1 \frac{m_B}{\sqrt{2}}, b_1\right) + \frac{5}{3} \int_{1/b_1}^t \frac{d\bar{\mu}}{\bar{\mu}} \gamma_q(\alpha_s(\bar{\mu})), \quad (\text{A9})$$

$$S_G(t) = s_G\left(x_2 \frac{\rho m_B}{\sqrt{2}}, b_2\right) + s_G\left((1 - x_2) \frac{\rho m_B}{\sqrt{2}}, b_2\right), \quad (\text{A10})$$

where the explicit form for the function  $s_G(Q, b)$  is

$$s_G(Q, b) = \int_{1/b}^Q \frac{d\mu}{\mu} \left[ \ln\left(\frac{Q}{\mu}\right) A(\alpha(\mu)) \right], \quad A = \frac{\alpha_s}{\pi} C_A, \quad (\text{A11})$$

with  $C_A = 3$ . Since there is no endpoint singularity in these diagrams, the contribution from the endpoint region will not be large and we will neglect the jet function arising from the threshold resummation. We adopt the one-loop expression of the running coupling constant  $\alpha_s$ , when evaluating the above Sudakov factors

- 
- [1] G. S. Bali, *et al.* [UKQCD Collaboration], Phys. Lett. B **309**, 378 (1993);  
H. Chen, J. Sexton, A. Vaccarino and D. Weingarten, Nucl. Phys. Proc. Suppl. **34**, 357 (1994);  
C. J. Morningstar and M. J. Peardon, Phys. Rev. D **60**, 034509 (1999) ;  
A. Vaccarino and D. Weingarten, Phys. Rev. D **60**, 114501 (1999) ;  
C. Liu, Chin. Phys. Lett. **18**, 187 (2001) ;  
D. Q. Liu, J. M. Wu and Y. Chen, High Energy Phys. Nucl. Phys. **26**, 222 (2002) ;  
N. Ishii, H. Suganuma and H. Matsufuru, Phys. Rev. D **66**, 014507 (2002); Phys. Rev. D **66**, 094506 (2002);  
M. Loan, X. Q. Luo and Z. H. Luo, Int. J. Mod. Phys. A **21**, 2905 (2006) ;
- [2] Y. Chen *et al.*, Phys. Rev. D **73**, 014516 (2006) [arXiv:hep-lat/0510074].
- [3] S. Spanier, N.A. Törnqvist, and C. Amsler, note on scalar mesons, review published on particle data group.
- [4] P. Minkowski and W. Ochs, Eur. Phys. J. C **39**, 71 (2005) [arXiv:hep-ph/0404194];  
P. Minkowski and W. Ochs, arXiv:hep-ph/0304144.
- [5] X. G. He and T. C. Yuan, arXiv:hep-ph/0612108.
- [6] C. H. Chen and T. C. Yuan, Phys. Lett. B **650**, 379 (2007) [arXiv:hep-ph/0702067].
- [7] Y. Y. Charng, T. Kurimoto and H. n. Li, Phys. Rev. D **74**, 074024 (2006) [Phys. Rev. D **78**, 059901 (2008)] .

- [8] Y. Y. Keum, H. n. Li and A. I. Sanda, Phys. Lett. B **504**, 6 (2001); Phys. Rev. D **63**, 054008 (2001) ;
- [9] C. D. Lu, K. Ukai and M. Z. Yang, Phys. Rev. D **63**, 074009 (2001); C.D.-Lu and M.-Z.Yang, Eur. Phys. J. C23, 275-287 (2002); e-Print: hep-ph/0011238.
- [10] M. Beneke, G. Buchalla, M. Neubert and C. T. Sachrajda, Nucl. Phys. B **591**, 313 (2000) .
- [11] A. G. Grozin and M. Neubert, Phys. Rev. D**55**, 272 (1997) [hep-ph/9607366]; M. Beneke amd T. Feldmann, Nucl. Phys. B **592**, 3 (2001) [hep-ph/0008255].
- [12] H. Kawamura, J. Kodaira, C. F. Qiao and K. Tanaka, Phys. Lett. B**523**, 111(2001); B **536**, 344 (2002) (E) [hep-ph/0109181]; Mod. Phys. Lett. A**18**, 799 (2003) [hep-ph/0112174].
- [13] Z. T. Wei and M. Z. Yang, Nucl. Phys. B **642**, 263 (2002) [arXiv:hep-ph/0202018].
- [14] C. D. Lu and M. Z. Yang, Eur. Phys. J. C **28**, 515 (2003) [arXiv:hep-ph/0212373].
- [15] X. G. He, H. Y. Jin and J. P. Ma, Phys. Rev. D **66**, 074015 (2002) [arXiv:hep-ph/0203191].
- [16] V. M. Braun, G. P. Korchemsky and D. Mueller, Prog. Part. Nucl. Phys. **51**, 311 (2003) [arXiv:hep-ph/0306057].
- [17] A. Ali, et al., Phys. Rev. D**76**, 074018 (2007) e-Print: hep-ph/0703162.
- [18] W. Wang, Y. L. Shen, Y. Li and C. D. Lu, Phys. Rev. D **74**, 114010 (2006) [arXiv:hep-ph/0609082].
- [19] R. H. Li, C. D. Lu, W. Wang and X. X. Wang, Phys. Rev. D **79**, 014013 (2009) [arXiv:0811.2648 [hep-ph]] .
- [20] H. Y. Cheng, C. K. Chua and K. C. Yang, Phys. Rev. D **73**, 014017 (2006) [arXiv:hep-ph/0508104].
- [21] S. Descotes-Genon and C. T. Sachrajda, Nucl. Phys. B **625**, 239 (2002) [arXiv:hep-ph/0109260].
- [22] H. n. Li and H. S. Liao, Phys. Rev. D **70**, 074030 (2004) [arXiv:hep-ph/0404050].
- [23] For a review, see G. Buchalla, A. J. Buras and M. E. Lautenbacher, Rev. Mod. Phys. **68**, 1125 (1996) [arXiv:hep-ph/9512380].
- [24] A. J. Buras and M. Munz, Phys. Rev. D **52**, 186 (1995) [arXiv:hep-ph/9501281].
- [25] C. Amsler *et al.* [Particle Data Group], Phys. Lett. B **667**, 1 (2008).
- [26] J. Charles *et al.* [CKMfitter Group], Eur. Phys. J. C **41**, 1 (2005) [arXiv:hep-ph/0406184]. The updated results can be found at <http://ckmfitter.in2p3.fr/>.
- [27] B. Aubert *et al.* [BABAR Collaboration], arXiv:0808.3524 [hep-ex].
- [28] C. Amsler and F. E. Close, Phys. Lett. B **353**, 385 (1995) [arXiv:hep-ph/9505219];  
C. Amsler and F. E. Close, Phys. Rev. D **53**, 295 (1996) [arXiv:hep-ph/9507326].
- [29] F. E. Close and A. Kirk, Phys. Lett. B **483**, 345 (2000) [arXiv:hep-ph/0004241];  
F. E. Close and Q. Zhao, Phys. Rev. D **71**, 094022 (2005) [arXiv:hep-ph/0504043].
- [30] H. Y. Cheng, C. K. Chua and K. F. Liu, Phys. Rev. D **74**, 094005 (2006) [arXiv:hep-ph/0607206].
- [31] B. H. Hong and C. D. Lu, Sci. China **G49**, 357 (2006) [arXiv:hep-ph/0505020].
- [32] H. n. Li, Phys. Lett. B **622**, 63 (2005) [arXiv:hep-ph/0411305].
- [33] M. Nagashima and H. n. Li, Phys. Rev. D **67**, 034001 (2003) [arXiv:hep-ph/0210173].
- [34] Y. Liu *et al.* [Belle Collaboration], Phys. Rev. D **78**, 011106 (2008) [arXiv:0805.3225 [hep-ex]].
- [35] F. De Fazio and M. R. Pennington, Phys. Lett. B **521**, 15 (2001) [arXiv:hep-ph/0104289].
- [36] K. Monig, hep-ex/0101005.